

INTERNATIONAL SOCIETY FOR SOIL MECHANICS AND GEOTECHNICAL ENGINEERING



This paper was downloaded from the Online Library of the International Society for Soil Mechanics and Geotechnical Engineering (ISSMGE). The library is available here:

<https://www.issmge.org/publications/online-library>

This is an open-access database that archives thousands of papers published under the Auspices of the ISSMGE and maintained by the Innovation and Development Committee of ISSMGE.

An elasto-plastic constitutive model for structured sand with interparticle bonding

Un modèle constitutif élastoplastique pour du sable structuré avec liaison d'interparticules

D. Katsuki

Gas Hydrate Group, Energy Technology Research Institute,
 National Institute of Advanced Industrial Science and Technology (AIST), Sapporo, Japan

Y. Nakata

Faculty of Engineering, Yamaguchi University, Ube, Japan

ABSTRACT

A constitutive equation of sand in which the particles are weakly bonded at contact was proposed. The proposed equation was developed on the basis of critical state and subloading surface concepts. The effect of bonding on the mechanical behavior of sand was quantified as an internal stress component. The degradation of bonding caused by loading was modeled as an evolution law of the internal stress. Analysis of the specifics of internal stress degradation played an indispensable role in developing a valid model of bonded sand.

RÉSUMÉ

Une équation constitutive de sable dans lequel des particules sont faiblement liées à des contacts a été proposée. L'équation constitutive proposée a été mise au point sur la base d'une condition critique et de concepts d'une surface de sous-chargement. L'effet de la liaison sur le comportement mécanique du sable a été quantifié en tant qu'élément de contrainte interne. La dégradation de la liaison provoquée par le chargement a été modélisée comme une loi de l'évolution d'une contrainte interne. La dégradation de cette contrainte interne joue un rôle indispensable dans une modélisation appropriée du sable lié.

1 INTRODUCTION

Many laboratory tests have been performed on various bonded sands (Lade & Overton, 1989; Cuccovillo & Coop, 1999; Ismail, 2000). The results suggest that many common mechanical properties exist among bonded sands of different origin (Leroueil & Vaughan, 1990). The common properties were taken as the greater compressive yield stress, the peak angle of shearing resistance and the positive dilatancy for the bonded sand than non-bonded one (Lade & Overton, 1989). These differences in properties can be attributed to the effect of bonding. The behavior of bonded sand returns to that of non-bonded sand through loading (Leroueil & Vaughan, 1990). Quantifying the bonding effect is a rational method of describing the mechanical behavior of various bonded sands. Furthermore, the effect of bonding should be treated as an additional component because it is always degraded during loading. The above-mentioned approach was insufficient, although some constitutive models have been proposed (Lagioia & Nova, 1995; Kasama et al., 2000; Kavvasdas & Amorosi, 2000). Therefore further studies are necessary to understand and describe the comprehensive property of various bonded sands.

The constitutive equation presented in this paper quantifies the effect of bonding as an internal stress component. Furthermore, the degradation of bonding has been modeled as an evolution law of the internal stress component. Applicability of the equation to a laboratory test on bonded carbonate sand has been verified. Finally, the significance of the presented modeling approaches is discussed on the basis of a parametric study.

2 CONSTITUTIVE LAW OF BONDED SAND

The following discussion is restricted to an axisymmetric stress condition. The stress and strain increment parameters used are given by

$$p = (\sigma_a + 2\sigma_r)/3, \quad q = \sigma_a - \sigma_r \quad (1)$$

$$d\varepsilon_v = d\varepsilon_a + 2d\varepsilon_r, \quad d\varepsilon = 2(d\varepsilon_a - d\varepsilon_r)/3 \quad (2)$$

where σ_a and σ_r are the axial (maximum) and radial (minimum) effective principal stresses and, $d\varepsilon_a$ and $d\varepsilon_r$ are the axial and radial strain increments. Each of the strain increments is given as the sum of the elastic and the plastic strain increments. Each plastic strain increment is given by

$$d\varepsilon_v^p = \Lambda \frac{\partial g}{\partial p}, \quad d\varepsilon^p = \Lambda \frac{\partial g}{\partial q} \quad (3)$$

where Λ is a positive scalar parameter and, g is the plastic potential. Interparticle bonding is thought to provide additional resistance to sliding between particles. Such additional resistance is assumed to be replaced with frictional resistance arising from internal stresses. The effect of internal stress can be imagined to be similar to that of suction. It is conceptually rational that internal stress is given as a sum of an "internal force" caused by each interparticle bond within a unit cross-section. In the axisymmetric stress condition, internal stress can be specified with an axial and a radial internal stress components, $\sigma_{a,int}$ and $\sigma_{r,int}$. If the true effective stress is given by the sum of the external stress and the internal stress, then the hydrostatic and deviatoric true effective stresses are given as

$$p_t = p + (\sigma_{a,int} + 2\sigma_{r,int})/3, \quad q_t = q + (\sigma_{a,int} - \sigma_{r,int}) \quad (4a)$$

If the sand possesses fabric isotropy, $\sigma_{a,int} = \sigma_{r,int}$ can be assumed. Eq. 4a is therefore reduced to

$$p_t = p + p_{int}, \quad q_t = q \quad (4b)$$

where $p_{int} = (\sigma_{a,int} + 2\sigma_{r,int})/3$. The parameter p_{int} is called "internal stress".

Fig. 1 presents a compression curve of the bonded sand that possesses constant internal stress during compression. The normal compression line (NCL) of bonded sand is assumed to be parallel to that of non-bonded sand, and is then defined as

$$e = e_c(p_{int}) - \lambda \ln p \quad (5)$$

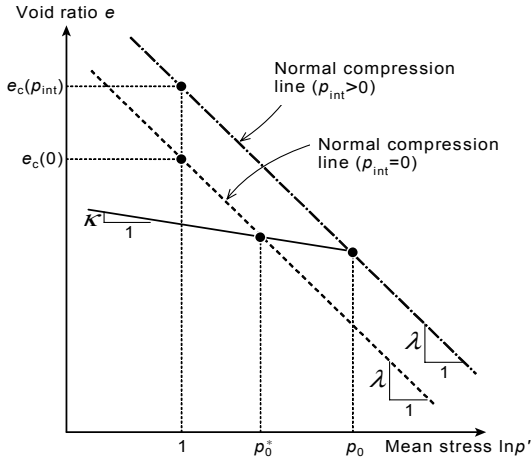


Figure 1. Compression property of the bonded sand having constant p_{int}

where $e_c(p_{int})$ is a void ratio on the NCL at a unit stress. The parameter $e_c(p_{int})$ is assumed to be given by

$$e_c(p_{int}) = e_c(0) + \frac{p_{int}}{\alpha + \beta p_{int}} \quad (6)$$

where $e_c(0)$ is the void ratio on NCL of the non-bonded sand (i.e. $p_{int} = 0$) at unit stress, α and β are material constants. According to Eq. 5 and Eq. 6, a yield surface in (p, p_{int}) plane is defined as

$$p_0 = p_0^* \exp\left\{\frac{p_{int}}{(\lambda - \kappa)(\alpha + \beta p_{int})}\right\} \quad (7)$$

where p_0^* is the isotropic compression yield stress of sand in the non-bonded state. In reference to Kasama et al. (2000), the dissipated energy equation of bonded sand is defined as

$$p d\varepsilon_v^p + q d\varepsilon^p = (p + p_{int}) \sqrt{(d\varepsilon_v^p)^2 + (M d\varepsilon^p)^2} - p_{int} d\varepsilon_v^p \quad (8)$$

where M is the critical stress ratio of the sand. If the bonding disappears (i.e. $p_{int} = 0$), Eq. 8 is reduced to the dissipated energy equation of the modified Cam-clay model (Roscoe and Burland, 1968). The stress-dilatancy relationship of the bonded sand is derived as

$$\frac{d\varepsilon_v^p}{d\varepsilon^p} = \frac{M^2 - \eta^{*2}}{2\eta^*} \quad (9)$$

where $\eta^* = q / (p + p_{int})$. By applying the normality rule to Eq. 9, the plastic potential g is obtained as

$$g: \ln(p + p_{int}) + \ln(\eta^{*2} + M^2) = const. \quad (10)$$

The normal yield surface that defines a normal yield state is assumed to be given by

$$F: (p + p_{int}) \exp\left(\frac{\eta^{*2}}{2N^2}\right) = (p_0 + p_{int}) \quad (11)$$

where N is a material constant specifying a shape of the surface. After Hashiguchi and Ueno (1977), the sub-loading surface that is similar to the normal yield surface is introduced as

$$f: (p + p_{int}) \exp\left(\frac{\eta^{*2}}{2N^2}\right) = R(p_0 + p_{int}) \quad (12)$$

where R is the similarity ratio of the sub-loading surface to the normal yield surface ($R \leq 1$). Fig. 2 shows a schematic diagram of the yield surface presented as Eq. 7, the normal yield surface (Eq. 11), the plastic potential (Eq. 10) and the sub-loading surface (Eq. 12) in (p, q, p_{int}) stress space.

The evolution law of the similarity ratio R is defined as

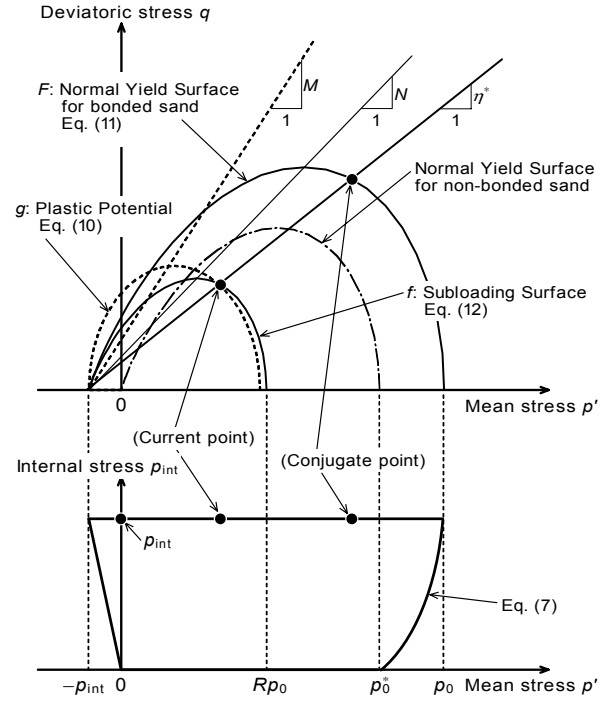


Figure 2. A schematic diagram of the normal yield surface F , the sub-loading surface f and the plastic potential g

$$dR = U_R \sqrt{(d\varepsilon_a^p)^2 + 2(d\varepsilon_r^p)^2} \quad (13)$$

where U_R is a monotonically decreasing function. It is given by

$$U_R = -u \ln R \quad (14)$$

where u is a material constant. In light of the degradation of bonding with increasing plastic deformation, the evolution law of the internal stress is assumed to be given by

$$dp_{int} = -\chi p_{int} \sqrt{(d\varepsilon_v^p)^2 + (M d\varepsilon^p)^2} \quad (15)$$

where χ is a material constant. On the assumption of isotropic hardening for the sand, the hardening-softening law is given as

$$dp_0 = \frac{\partial p_0}{\partial p_0^*} \frac{\partial p_0^*}{\partial \varepsilon_v^p} \Lambda \frac{\partial g}{\partial p} + \frac{\partial p_0}{\partial p_{int}} dp_{int} \quad (16)$$

From the consistency condition on the sub-loading surface, the positive scalar Λ is given by

$$\Lambda = \frac{1}{H} \left(\frac{\partial f}{\partial p} dp + \frac{\partial f}{\partial q} dq \right) \quad (18)$$

where H is the hardening modulus. H is expressed as

$$H = U_R \sqrt{\left(\frac{\partial g}{\partial \sigma_a}\right)^2 + 2\left(\frac{\partial g}{\partial \sigma_r}\right)^2} (p_0 + p_{int}) + R \frac{\partial p_0}{\partial p_0^*} \frac{\partial p_0^*}{\partial \varepsilon_v^p} \frac{\partial g}{\partial p} - \chi p_{int} \left\{ R \left(\frac{\partial p_0}{\partial p_{int}} + 1 \right) - \frac{\partial f}{\partial p_{int}} \right\} \sqrt{\left(\frac{\partial g}{\partial p}\right)^2 + \left(M \frac{\partial g}{\partial q}\right)^2} \quad (19)$$

The total strain increments $d\varepsilon$, and $d\varepsilon$ are given by

$$\begin{pmatrix} d\varepsilon_v \\ d\varepsilon \end{pmatrix} = \begin{bmatrix} \frac{1}{K} & 0 \\ 0 & \frac{1}{3G} \end{bmatrix} \begin{pmatrix} dp \\ dq \end{pmatrix} + \Lambda \begin{pmatrix} \frac{\partial g}{\partial p} \\ \frac{\partial g}{\partial q} \end{pmatrix} \quad (20)$$

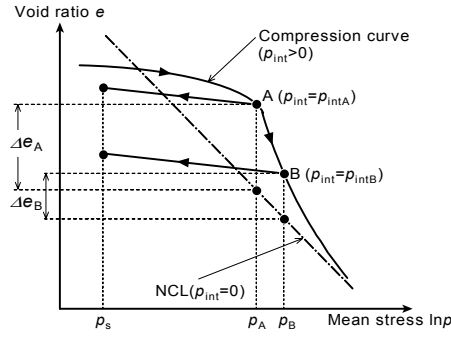


Figure 3. Stress path for determination of the material constants α and β

3 DETERMINATION OF INTERNAL STRESS AND MATERIAL CONSTANTS

The internal stress p_{int} can be determined from a conventional triaxial compression test on bonded sand at a low confining pressure. The following equation is obtained by solving Eq. 9 for p_{int} at $-d\varepsilon_v^p/d\varepsilon^p = 0$,

$$p_{int} = (q_{pt}/M) - p_{pt} \quad (21)$$

where p_{pt} and q_{pt} are the mean and the deviatoric stresses at which the strain increment ratio $-d\varepsilon_v^p/d\varepsilon^p$ is equal to 0. For engineering purpose, the total strain increment ratio $-d\varepsilon_v/d\varepsilon$ can be substituted for $-d\varepsilon_v^p/d\varepsilon^p$. The degradation of bonding at the state of $-d\varepsilon_v/d\varepsilon = 0$ is thought to be small since a confining pressure applied is low and the state of $-d\varepsilon_v/d\varepsilon = 0$ has not yet reached peak. Therefore, the internal stress determined as stated above can be regarded as the initial internal stress p_{int0} .

A total of nine material constants characterize the constitutive relationship. The constants can be determined as follows. The constants λ , κ and $e_c(0)$, which specify the compression property of the sand, are derived from isotropic compression/swelling tests on the non-bonded sand. λ and κ are the slope of the normal compression line and the swelling line. $e_c(0)$ is the void ratio on the NCL at a unit stress. The critical stress ratio M is obtained from a triaxial compression test on the non-bonded sand. The constant N is determined from the following stress path test on the non-bonded sand. After the non-bonded sand is isotropically loaded up to $p = p_0$, it is unloaded and sheared to specify the yield stresses p_y and q_y corresponding to p_0 . Finally, N is obtained from

$$N = \frac{q_y}{p_y} \left(2 \ln \frac{p_0}{p_y} \right)^{-1/2} \quad (22)$$

which is derived from Eq. 11. The constants α and β are determined as follows. A typical isotropic compression curve of bonded sand is shown in Fig. 3. "A" indicates the point at which $\Delta e (= e_{bonded} - e_{NCL})$ reaches maximum. After the bonded sand is loaded up to p_A , it is unloaded down to a low stress p_s and then sheared to assess the internal stress at p_A . Additionally, another bonded specimen is subjected to the similar test; the only difference is that the pre-compression stress p_B is larger than p_A . Finally, α and β can be determined by fitting Eq. 6 to the $\Delta e_A - p_{intA}$ and $\Delta e_B - p_{intB}$ relationships. χ on which the degradation rate of the internal stress is dependent is determined from

$$\chi = - \frac{\ln(p_{intA}/p_{int0})}{\varepsilon_{vA}^p} \quad (23)$$

where ε_{vA}^p and p_{intA} are the plastic volumetric strain and the internal stress at p_A . The constant u characterizes the evolution law of the similarity ratio dR . The constant u can be determined by curve-fitting the computed isotropic compression curve to the experimental data using other determined material constants.

Table 1. Index properties of Rottenest sand (after Ismail, 2000)

G_s	D_{50} mm	Fine content %	e_{max}	e_{min}
2.70	0.30	0.8	1.231	0.824

Table 2. Material constants and the initial internal stress used for Rottenest sand and the parametric study in Sec. 5.

	Rottenest sand	Sand _A , Sand _B (in Sec. 5)
$e_c(0)$	1.13	1.10
λ	0.192	0.150
κ	0.0055	0.0055
M	1.59	1.20
N	0.96	1.0
α	5.71	2.5
β	0.980	5.0
χ	23.1	40.0
u	$Q_c' = 0\%$, 30 $Q_c' = 3.5\%$, 120	Sand _A , 30 Sand _B , 120
p_{int0}	$Q_c' = 0\%$, 0 MPa $Q_c' = 3.5\%$, 0.130 MPa	Sand _A , 0 MPa Sand _B , 0.30 MPa

4 APPLICABILITY TO A LABORATORY TEST

Ismail (2000) prepared bonded sand specimens by permeating CaCO_3 solution through the previously packed carbonate sand (Rottenest sand, referred to as RT sand). A microscopic observation showed that the particles in the bonded RT sand were bonded at contacts via the precipitations of CaCO_3 . Ismail (2000) mentioned that these bonded sands are capable of simulating the mechanical behavior of undisturbed bonded carbonate sands. Table 1 lists the index properties of the RT sand. RT sand is relatively high in both the maximum and the minimum void ratios. This feature is typically found in other carbonate sands and arises from irregularity of grain shape. Data from a triaxial compression test on both the non-bonded RT sand and the bonded RT sand with CaCO_3 cement content ($Q_c' = (M_{\text{CaCO}_3}/M) \times 100\%$) of 3.5% was referenced to verify the applicability of the proposed constitutive equation. Material constants and initial internal stress of the RT sand were determined as listed in Table 2. Incidentally, the constants α and β could not be determined as described above due to lack of available data. Therefore, Eq. 6 was resolved using data from isotropic compression tests on the two bonded sands of $Q_c' = 7\%$ and 9% . Then, it is assumed that 50% of the internal stress for the bonded sand of $Q_c' = 7\%$ and 40% of the internal stress for the bonded sand of $Q_c' = 9\%$ have been lost at each point of maximum Δe . Although the estimated magnitude of the internal stress loss is uncertain, the relative magnitude between the two bonded sands is reliable. Since the magnitude of loss is a function of the plastic volumetric strain alone during isotropic compression as shown in Eq. 23, the relative one can be determined from each volumetric strain.

Fig. 4(a) shows the stress-strain behavior of the constant p test on both the non-bonded and bonded RT sands (Ismail, 2000). The computed stress-strain behavior is shown in Fig. 4(b). The phenomenon that the relationship between stress ratio and deviatoric strain of the bonded sand approaches that of the non-bonded sand at $p = 0.5$ MPa is seen in the computed data over a deviatoric strain of 6%. It is also demonstrated that dilatancy of the bonded sand is higher than that of the non-bonded sand, although the difference between the bonded and the non-bonded sands is small. The transitional stress-strain behavior of the bonded sand, which varies from strain softening to strain hard-

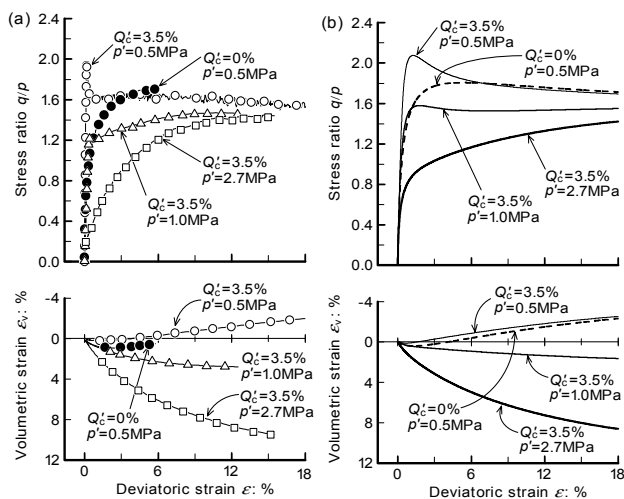


Figure 4. Verification of applicability to a laboratory test: (a) experimental data of RT sand (after Ismail, 2000); (b) computed data

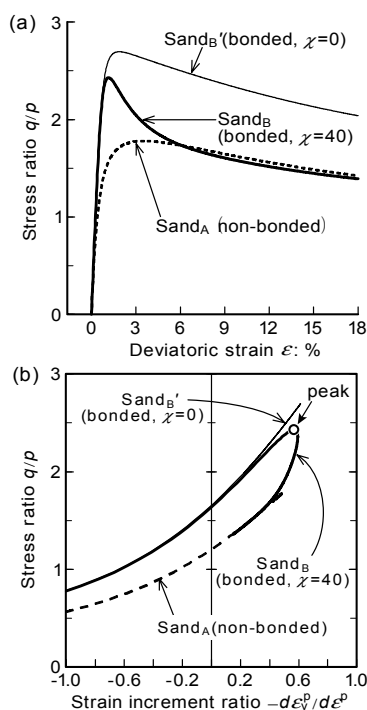


Figure 5. Effect of degradation on computed behavior: (a) stress-strain behavior; (b) stress-dilatancy relationship

ening with increasing mean stress, is also appropriately represented. Incidentally, for all computed data, the residual stress ratios will approach the value of M eventually, although the stress ratios of the data in Fig. 4(b) do not yet reach it at $\varepsilon = 18\%$.

5 EFFECT OF DEGRADATION ON COMPUTED BEHAVIOR

The effect of degradation on computed behavior was studied. It is supposed that $Sand_A$ and $Sand_B$ represent a non-bonded sand and a bonded sand, respectively. These imaginary sands are characterized in Table 2. Fig. 5(a) and 5(b) show the stress-strain relationship and the stress-dilatancy relationship computed under a constant mean stress of 0.8 MPa. Note that the data for $Sand_B'$ in Fig 5 has been computed with the material constant χ of 0, namely without degradation ($p_{int} = p_{int0}$). It was experimentally observed that dilatancy of a bonded sand was higher than that of a non-bonded sand (Lade and Overton, 1989). As shown in Fig. 5(b), the proposed model can characterize the

effect of bonding on dilatancy. Comparing $Sand_B$ to $Sand_B'$ clarifies the effect of degradation on the constitutive relationship. Both the peak stress ratio and the stress ratio during softening of $Sand_B'$ are higher than those of $Sand_B$. In addition, the relationship between stress ratio and deviatoric strain of $Sand_B$ approaches that of the non-bonded sand ($Sand_A$) after strong strain softening. In Fig. 5(b), the stress-dilatancy relationship of $Sand_B'$ has returned along the same path after the peak. In contrast, the stress-dilatancy relationship of $Sand_B$ gradually deviates from that of $Sand_B'$ before the peak. After the peak it coincides with that of $Sand_A$ as the internal stress is degraded. The above parametric study has clarified that the proposed constitutive equation can describe the effects of bonding, such as an increase in shearing resistance with increasing dilatancy rate, via the internal stress component. Furthermore, we have also concluded that the concept of degradation of the internal stress is necessary for appropriately demonstrating the behavior of bonded sand. These modelling approaches are considered to be suitable for a variety of weakly bonded sands that predominantly consist of sand grains.

6 SUMMARY AND CONCLUSIONS

The essentials of the modeling approach presented in this paper and the conclusions derived from the computational study are listed below.

- A constitutive equation of bonded sand was proposed on the basis of the following approaches. An internal stress component was introduced to quantify the effects of bonding on the mechanical behavior of sand. In addition, in order to define the degradation of bonding, an evolution law of the internal stress was defined as a function of the plastic strain increments.
- The proposed constitutive equation could describe the mechanical behavior of a weakly bonded carbonate sand. Most importantly, it suitably represented the changes in behavior caused by both the development and the degradation of bonding.
- The modeling approaches presented, which quantified the bonding effect as the internal stress component and specified the characteristics of degradation, could be considered a valid approach in the analysis and description of various weakly bonded sands.

REFERENCES

- Cuccovillo, T. and Coop, M.R. 1999. On the mechanics of structured sands, *Géotechnique*, Vol. 49, No. 6, 741–760.
- Hashiguchi, K. and Ueno, M. 1977. Elastoplastic constitutive laws of granular materials, *Constitutive Equations of Soils, Proc. 9th Int. Conf. Soil Mech. Found. Eng., Spec. Ses. 9*, Murayama, S. and Schofield, A. N. (Eds), Tokyo, JSSMFE, 73–82.
- Ismail, M.A. 2000. Strength and deformation behaviour of calcite-cemented calcareous soil, *PhD thesis of The University of Western Australia*.
- Kasama, K., Ochiai, H. and Yasufuku, N. 2000. On the stress-strain behaviour of lightly cemented clay based on an extended critical state concept, *Soils and Foundations*, Vol. 40, No. 5, 37–47.
- Kavvas, M. and Amorosi, A. 2000. A constitutive model for structured soils, *Géotechnique*, Vol.50, No. 3, 263–273.
- Lade, P.V. and Overton, D.D. 1989. Cementation effects in frictional materials, *J. of Geotech. Engrg., ASCE*, Vol. 115, No. 10, 1373–1387.
- Lagioia, R. and Nova, R. 1995. An experimental and theoretical study of the behaviour of a calcarenite in triaxial compression, *Géotechnique*, Vol. 45, No. 4, 633–648.
- Leroueil, S. and Vaughan, P.R. 1990. The general and congruent effects of structure in natural soils and weak rocks, *Géotechnique*, Vol. 40, No. 3, 467–488.
- Roscoe, K.H. and Burland, J.B. 1968. On the generalized stress strain behaviour of “wet” clay, *Engineering Plasticity*, Cambridge Univ. Press, 535–609.